Pramana – J. Phys. (2021) 95:162
https://doi.org/10.1007/s12043-021-02187-w

Cluster pre-formation probabilities and decay half-lives for trans-lead nuclei using modified generalised liquid drop model (MGLDM)

K P SANTHOSH* and TINU ANN JOSE

School of Pure and Applied Physics, Kannur University, Swami Anandatheertha Campus, Payyanur 670 327, India
*Corresponding author. E-mail: drkpsanthosh@gmail.com

MS received 22 June 2019; revised 28 October 2020; accepted 6 May 2021

Abstract. Cluster decay half-lives of trans-lead nuclei emitting clusters like C, N, O, F, Ne, Mg and Si are studied by incorporating various cluster pre-formation probabilities to the modified generalised liquid drop model (MGLDM). MGLDM is a method in which generalised liquid drop model (GLDM) is modified using proximity 77 potential. In this approach, we make the assumption that the cluster is pre-born inside the parent nuclei and the pre-formation factor that depends on Q value, size of the cluster and product of atomic number of the cluster and the daughter nuclei are formulated and added to MGLDM. Calculated half-lives using three formulae are cross checked with experimentally detected values from various isotopes of Fr, Ra, Ac, Th, U, Pa, Np, Pu and Am parent nuclei and the results match exactly. Standard deviations of logarithmic half-lives using pre-formation factors which depend on Q values, cluster size and product of atomic number of the cluster and the daughter nuclei, are 1.08, 0.995 and 1.07 respectively. Hence, we formulate a pre-formation factor that depends on all the three parameters together in an equation and the standard deviation is found to be 0.885. Again, the four formulae proved its applicability in the case of alpha decay from the parent nuclei of atomic numbers 85–102.

Keywords. Cluster radioactivity; alpha radioactivity; half-life.

PACS Nos **23.70.+j; 23.60.+e; 27.90.+b**

1. Introduction

Cluster radioactivity, a decay event that emits particles heavier than alpha particle but lighter than fission fragments, was first predicted by Săndulescu *et al* [1]. First experimental observation of this prediction was done by Rose and Jones [2] and later by Aleksandrov *et al* [3]. After that, the emission of other clusters like ^{20}O, ^{23}F, ^{22,24,26}Ne, ^{28,30}Mg, ^{32,34}Si were observed experimentally from different parents [4,5]. Thereafter, experimental detection of various heavier clusters in trans-lead region leading to stable daughter nuclei around ^{208}Pb were observed [6–12].

Cluster is a particle intermediate in size between alpha and fission fragments. After its prediction and experimental detection, the main aim of the researchers was to explain the reason or basic theory behind its emission. Many theoretical models were suggested and almost all models treated cluster decay in two ways–with and without including pre-formation factor; the one which included pre-formation concept is the pre-formed cluster model [13–15] where cluster is pre-born within the parent nuclei before emission and the other which neglected the concept of pre-formation is the superasymmetric fission model [16–19].

Among several theoretical approaches, liquid drop model (LDM) with certain modification was found to be a reasonable approach that could explain cluster emission to a great extent. To the conventional LDM, Royer *et al* [19–26] included nuclear proximity energy and quasimolecular shape, thereby proposing generalised liquid drop model (GLDM). In 1998, cluster decay half-lives by GLDM was calculated [18]. Then Bao *et al* [27] modified LDM by adding the influence of microscopic shell correction and shape-dependent pairing energy to it. Santhosh *et al* used proximity potential 77 of Blocki *et al* [28] in different models [29] and then later improved GLDM of Royer *et al* [19–26] by considering proximity potential 77 as the potential barrier, which is termed as MGLDM [30]. In this approach, experimental and predicted values agree fairly well.

Published online: 05 October 2021

We assume the cluster to be born within the parent nuclei before it is emitted. Hence, the parameter on which the cluster pre-formation probability depends, plays a dominant role. It is clearly understood that the disintegration constant depends on pre-formation factor of the particle to be emitted. Hence, in the pre-formed cluster model, an additional pre-formation factor (P_c) is multiplied with assault frequency (ν_0) and barrier penetrability constant (P) to get decay constant [31–34] unlike in the unified fission model [35–38]. Based on these structural factors, several formulae were also developed [39–44] to determine the cluster pre-formation probability. Blendowske and Walliser [39] deduced an expression for pre-formation parameter that depends on the pre-formation factor of alpha particle and size of the cluster in which deviation was about two orders of magnitude. Ni *et al* [40] proposed an expression that depends on the reduced mass and product of charge numbers of the cluster and the daughter nuclei. Balasubramanian *et al* [41] proposed different empirical relations in terms of Q value, mass asymmetry and cluster size. Ren *et al* [42] proposed an expression that depends on multiplicity of charges. From the observed variation of pre-formation probability with isospin asymmetry, we obtained an expression [44] for pre-formation probability and studied alpha and cluster decay of various isotopes. Recently, Santhosh *et al* [45] modified MGLDM by adding Q-dependent pre-formation parameters [46] and could replicate the observed result with minimum standard deviation. The quantities on which pre-formation probability depends and how it depends is very important. Correct dependence and correct expression may give experimentally matching results. Thus, it becomes essential to define an expression for the pre-formation factor based on the quantities on which it depends.

From several studies, it is evident that MGLDM is a successful approach in explaining the basic ideas of cluster emission. Moreover, pre-formation probability is something which cannot be neglected in the case of cluster decay. Hence, in this work, we modify MGLDM by adding three types of pre-formation factors that depend on Q value, size of the cluster and product of proton number of both the daughter and the emitted cluster and compares it with the observed values. As for the calculations, they could reproduce more or less the same values for the half-lives. Almost certainly, the pre-formation factor will be dependent upon all the three quantities. Hence, we use all the three parameters together to formulate an expression for pre-formation factor. Better matching results prove it as an accurate model and so we apply the same model in the case of alpha emission.

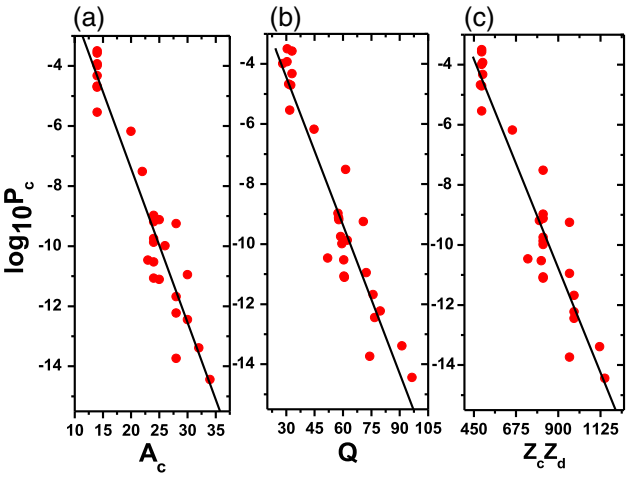

Figure 1. The variation of pre-formation factor (extracted from the experimental data) with the cluster size (**a**), with the Q value in decay (**b**) and with product of proton number of the cluster and the daughter nuclei (**c**).

The present paper is organised as: Section 2 gives the theory of MGLDM and discusses about various pre-formation factors. Section 3 includes results and discussion. Section 4 summarises the entire study.

2. Modified generalised liquid drop model (MGLDM)

In GLDM, for a deformed nucleus, the macroscopic energy is defined as

$$E = E_V + E_S + E_C + E_R + E_P. \tag{1}$$

Here the terms E_V, E_S, E_C, E_R and E_P represent the volume, surface, Coulomb, rotational and proximity energy terms respectively.

For the pre-scission region, the volume, surface and Coulomb energies in MeV are given by

$$E_V = -15.494(1 - 1.8I^2)A, \tag{2}$$

$$E_S = 17.9439(1 - 2.6I^2)A^{2/3}(S/4\pi R_0^2), \tag{3}$$

$$E_C = 0.6e^2(Z^2/R_0) \times 0.5 \int (V(\theta)/V_0)(R(\theta)/R_0)^3 \sin\theta \mathrm{d}\theta. \tag{4}$$

Here I is the relative neutron excess, S is the surface of the deformed nucleus, $V(\theta)$ is the electrostatic potential at the surface and V_0 is the surface potential of the sphere.

For the post-scission region,

$$E_V = -15.494\left[\left(1 - 1.8I_1^2\right)A_1 + \left(1 - 1.8I_2^2\right)A_2\right], \tag{5}$$

Table 1. Half-lives of ^{14}C cluster emission from various isotopes of Fr, Ra, Ac and Th using four types of pre-formation factors.

Cluster reaction	Q_c (MeV)	$\log_{10}[T_{1/2}(\mathrm{s})]$				
		$T_{1/2}^{(Q)}$	$T_{1/2}^{(A)}$	$T_{1/2}^{(Z)}$	$T_{1/2}^{(C)}$	Expt.
$^{216}\mathrm{Fr} \rightarrow {}^{14}\mathrm{C} + {}^{202}\mathrm{Tl}$	25.931	25.16	26.64	26.59	24.81	
$^{217}\mathrm{Fr} \rightarrow {}^{14}\mathrm{C} + {}^{203}\mathrm{Tl}$	27.057	22.48	23.71	23.66	22.28	
$^{218}\mathrm{Fr} \rightarrow {}^{14}\mathrm{C} + {}^{204}\mathrm{Tl}$	28.385	19.57	20.50	20.45	19.55	
$^{219}\mathrm{Fr} \rightarrow {}^{14}\mathrm{C} + {}^{205}\mathrm{Tl}$	29.419	17.45	18.16	18.11	17.58	
$^{220}\mathrm{Fr} \rightarrow {}^{14}\mathrm{C} + {}^{206}\mathrm{Tl}$	30.716	14.99	15.41	15.36	15.29	
$^{221}\mathrm{Fr} \rightarrow {}^{14}\mathrm{C} + {}^{207}\mathrm{Tl}$	31.291	13.93	14.23	14.18	14.31	14.52
$^{222}\mathrm{Fr} \rightarrow {}^{14}\mathrm{C} + {}^{208}\mathrm{Tl}$	30.108	16.00	16.55	16.50	16.22	
$^{223}\mathrm{Fr} \rightarrow {}^{14}\mathrm{C} + {}^{209}\mathrm{Tl}$	29.008	18.06	18.86	18.81	18.13	
$^{224}\mathrm{Fr} \rightarrow {}^{14}\mathrm{C} + {}^{210}\mathrm{Tl}$	27.976	20.13	21.15	21.10	20.05	
$^{225}\mathrm{Fr} \rightarrow {}^{14}\mathrm{C} + {}^{211}\mathrm{Tl}$	26.881	22.48	23.75	23.70	22.26	
$^{226}\mathrm{Fr} \rightarrow {}^{14}\mathrm{C} + {}^{212}\mathrm{Tl}$	26.051	24.37	25.83	25.78	24.04	
$^{216}\mathrm{Ra} \rightarrow {}^{14}\mathrm{C} + {}^{202}\mathrm{Pb}$	26.212	25.60	27.02	27.07	25.12	
$^{217}\mathrm{Ra} \rightarrow {}^{14}\mathrm{C} + {}^{203}\mathrm{Pb}$	27.657	22.22	23.32	23.36	21.94	
$^{218}\mathrm{Ra} \rightarrow {}^{14}\mathrm{C} + {}^{204}\mathrm{Pb}$	28.741	19.87	20.73	20.77	19.73	
$^{219}\mathrm{Ra} \rightarrow {}^{14}\mathrm{C} + {}^{205}\mathrm{Pb}$	30.144	17.07	17.62	17.66	17.12	
$^{220}\mathrm{Ra} \rightarrow {}^{14}\mathrm{C} + {}^{206}\mathrm{Pb}$	31.036	15.38	15.74	15.78	15.56	
$^{221}\mathrm{Ra} \rightarrow {}^{14}\mathrm{C} + {}^{207}\mathrm{Pb}$	32.396	13.00	13.06	13.10	13.36	13.39
$^{222}\mathrm{Ra} \rightarrow {}^{14}\mathrm{C} + {}^{208}\mathrm{Pb}$	33.049	11.90	11.82	11.86	12.34	11.01
$^{223}\mathrm{Ra} \rightarrow {}^{14}\mathrm{C} + {}^{209}\mathrm{Pb}$	31.828	13.85	14.04	14.08	14.14	15.20
$^{224}\mathrm{Ra} \rightarrow {}^{14}\mathrm{C} + {}^{210}\mathrm{Pb}$	30.535	16.09	16.56	16.60	16.20	15.68
$^{225}\mathrm{Ra} \rightarrow {}^{14}\mathrm{C} + {}^{211}\mathrm{Pb}$	29.466	18.07	18.77	18.81	18.03	
$^{226}\mathrm{Ra} \rightarrow {}^{14}\mathrm{C} + {}^{212}\mathrm{Pb}$	28.197	20.61	21.59	21.63	20.39	21.19
$^{227}\mathrm{Ra} \rightarrow {}^{14}\mathrm{C} + {}^{213}\mathrm{Pb}$	27.362	22.38	23.54	23.58	22.05	
$^{228}\mathrm{Ra} \rightarrow {}^{14}\mathrm{C} + {}^{214}\mathrm{Pb}$	26.103	25.26	26.71	26.75	24.76	
$^{229}\mathrm{Ra} \rightarrow {}^{14}\mathrm{C} + {}^{215}\mathrm{Pb}$	25.202	27.47	29.12	29.17	26.85	
$^{216}\mathrm{Ac} \rightarrow {}^{14}\mathrm{C} + {}^{202}\mathrm{Bi}$	25.865	27.59	29.08	29.22	26.88	
$^{217}\mathrm{Ac} \rightarrow {}^{14}\mathrm{C} + {}^{203}\mathrm{Bi}$	27.209	24.31	25.51	25.64	23.79	
$^{218}\mathrm{Ac} \rightarrow {}^{14}\mathrm{C} + {}^{204}\mathrm{Bi}$	28.466	21.49	22.40	22.54	21.14	
$^{219}\mathrm{Ac} \rightarrow {}^{14}\mathrm{C} + {}^{205}\mathrm{Bi}$	29.615	19.09	19.75	19.89	18.90	
$^{220}\mathrm{Ac} \rightarrow {}^{14}\mathrm{C} + {}^{206}\mathrm{Bi}$	30.752	16.87	17.29	17.42	16.83	
$^{221}\mathrm{Ac} \rightarrow {}^{14}\mathrm{C} + {}^{207}\mathrm{Bi}$	31.555	15.37	15.62	15.75	15.45	
$^{222}\mathrm{Ac} \rightarrow {}^{14}\mathrm{C} + {}^{208}\mathrm{Bi}$	32.471	13.76	13.80	13.94	13.95	
$^{223}\mathrm{Ac} \rightarrow {}^{14}\mathrm{C} + {}^{209}\mathrm{Bi}$	33.065	12.74	12.65	12.79	13.01	12.60
$^{224}\mathrm{Ac} \rightarrow {}^{14}\mathrm{C} + {}^{210}\mathrm{Bi}$	32.006	14.44	14.59	14.73	14.58	
$^{225}\mathrm{Ac} \rightarrow {}^{14}\mathrm{C} + {}^{211}\mathrm{Bi}$	30.476	17.13	17.61	17.75	17.06	17.16
$^{226}\mathrm{Ac} \rightarrow {}^{14}\mathrm{C} + {}^{212}\mathrm{Bi}$	29.407	19.15	19.86	20.00	18.93	
$^{227}\mathrm{Ac} \rightarrow {}^{14}\mathrm{C} + {}^{213}\mathrm{Bi}$	28.062	21.90	22.91	23.04	21.50	
$^{228}\mathrm{Ac} \rightarrow {}^{14}\mathrm{C} + {}^{214}\mathrm{Bi}$	27.076	24.06	25.29	25.42	23.52	
$^{229}\mathrm{Ac} \rightarrow {}^{14}\mathrm{C} + {}^{215}\mathrm{Bi}$	26.041	26.49	27.95	28.08	25.80	
$^{217}\mathrm{Th} \rightarrow {}^{14}\mathrm{C} + {}^{203}\mathrm{Po}$	26.497	27.10	28.46	28.69	26.31	
$^{218}\mathrm{Th} \rightarrow {}^{14}\mathrm{C} + {}^{204}\mathrm{Po}$	27.688	24.25	25.34	25.57	23.62	
$^{219}\mathrm{Th} \rightarrow {}^{14}\mathrm{C} + {}^{205}\mathrm{Po}$	28.971	21.42	22.22	22.45	20.97	
$^{220}\mathrm{Th} \rightarrow {}^{14}\mathrm{C} + {}^{206}\mathrm{Po}$	29.838	19.61	20.22	20.45	19.27	
$^{221}\mathrm{Th} \rightarrow {}^{14}\mathrm{C} + {}^{207}\mathrm{Po}$	31.066	17.22	17.57	17.80	17.05	
$^{222}\mathrm{Th} \rightarrow {}^{14}\mathrm{C} + {}^{208}\mathrm{Po}$	31.653	16.11	16.33	16.56	16.02	
$^{223}\mathrm{Th} \rightarrow {}^{14}\mathrm{C} + {}^{209}\mathrm{Po}$	32.732	14.20	14.19	14.42	14.26	
$^{224}\mathrm{Th} \rightarrow {}^{14}\mathrm{C} + {}^{210}\mathrm{Po}$	32.927	13.83	13.78	14.01	13.91	

Table 1. *Continued.*

Cluster reaction	Q_c (MeV)	$\log_{10}[T_{1/2}(\mathrm{s})]$				
		$T_{1/2}^{(Q)}$	$T_{1/2}^{(A)}$	$T_{1/2}^{(Z)}$	$T_{1/2}^{(C)}$	Expt.
$^{225}\mathrm{Th} \rightarrow {}^{14}\mathrm{C} + {}^{211}\mathrm{Po}$	31.723	15.83	16.04	16.27	15.76	
$^{226}\mathrm{Th} \rightarrow {}^{14}\mathrm{C} + {}^{212}\mathrm{Po}$	30.548	17.93	18.39	18.62	17.69	
$^{227}\mathrm{Th} \rightarrow {}^{14}\mathrm{C} + {}^{213}\mathrm{Po}$	29.439	20.05	20.75	20.98	19.66	
$^{228}\mathrm{Th} \rightarrow {}^{14}\mathrm{C} + {}^{214}\mathrm{Po}$	28.221	22.56	23.53	23.76	22.00	
$^{229}\mathrm{Th} \rightarrow {}^{14}\mathrm{C} + {}^{215}\mathrm{Po}$	27.107	25.03	26.25	26.48	24.32	
$^{230}\mathrm{Th} \rightarrow {}^{14}\mathrm{C} + {}^{216}\mathrm{Po}$	26.060	27.51	28.97	29.20	26.66	

$$E_S = 17.9439\left[\left(1 - 2.6I_1^2\right)A_1^{2/3} + \left(1 - 2.6I_2^2\right)A_2^{2/3}\right], \tag{6}$$

$$E_C = \frac{0.6e^2Z_1^2}{R_1} + \frac{0.6e^2Z_2^2}{R_2} + \frac{e^2Z_1Z_2}{r}. \tag{7}$$

Here A_i, Z_i, R_i and I_i are the masses, charges, radii and relative neutron excess of the fragments, r is the distance between the centres of the fragments.

The nuclear proximity potential E_P is given by Blocki *et al* [28] as

$$E_P(z) = 4\pi\gamma b\left[\frac{C_1C_2}{(C_1 + C_2)}\right]\Phi\left(\frac{z}{b}\right), \tag{8}$$

with the nuclear surface tension coefficient

$$\gamma = 0.9517\left[1 - 1.7826(N - Z)^2/A^2\right]\mathrm{MeV/fm^2}, \tag{9}$$

where N, Z and A represent neutron, proton and mass number respectively of the parent nucleus,Φ represents the universal proximity potential [47] given as

$$\Phi(\varepsilon) = -4.41\mathrm{e}^{-\varepsilon/0.7176}, \text{ for } \varepsilon > 1.9475, \tag{10}$$

$$\Phi(\varepsilon) = -1.7817 + 0.9270\varepsilon + 0.01696\varepsilon^2 - 0.05148\varepsilon^3, \text{ for } 0 \le \varepsilon \le 1.9475, \tag{11}$$

with $\varepsilon = z/b$, where the width (diffuseness) of the nuclear surface $b \approx 1$ fm and Süsmann central radii C_i of the fragments is related to sharp radii R_i as,

$$C_i = R_i - \left(\frac{b^2}{R_i}\right). \tag{12}$$

For R_i we use semiempirical formula in terms of mass number A_i as [47]

$$R_i = 1.28A_i^{1/3} - 0.76 + 0.8A_i^{-1/3}. \tag{13}$$

The barrier penetrability P is calculated with the action integral

$$P = \exp\left\{-\frac{2}{\hbar}\int_{R_{\mathrm{in}}}^{R_{\mathrm{out}}}\sqrt{2B(r)[E(r) - E(\mathrm{sphere})]}\mathrm{d}r\right\}, \tag{14}$$

where

$$R_{\mathrm{in}} = R_1 + R_2, \quad B(r) = \mu$$

and

$$R_{\mathrm{out}} = e^2Z_1Z_2/Q.$$

R_1, R_2 are the radii of the daughter nuclei and the emitted cluster respectively, μ is the reduced mass and Q is the released energy.

The partial half-life is related to the decay constant λ by

$$T_{1/2} = \left(\frac{\ln 2}{\lambda}\right) = \left(\frac{\ln 2}{\nu P_c P}\right). \tag{15}$$

The assault frequency ν has been taken as $10^{20}\,\mathrm{s}^{-1}$. P_c is the pre-formation factor.

2.1 *Pre-formation factor*

Pre-formation factor, which is the probability of a cluster to form inside the parent nuclei before emission, plays a crucial role in cluster decay. Pre-formation probability depends on the structural factors of both the emitted cluster and the daughter nuclei. To formulate an empirical formula for the pre-formation factor, variation of cluster pre-formation probabilities with various quantities like the size of the cluster, product of proton number of the cluster and the daughter nuclei, and the Q value for the decay have been studied. A graph is plotted with logarithm of pre-formation factor (extracted from experimental data) along the Y-axis and cluster size (A_c), energy released (Q) and product of proton number of the daughter nuclei and the cluster (Z_cZ_d) along the X-axis in figures 1a–1c respectively. From figure 1a, it is evident that the pre-formation probability decreases as the size of the cluster increases. Similar behaviour is obtained when the logarithm of pre-formation factor is plotted vs. Q value and product of proton number of the cluster and the daughter. Straight lines shown in the figure are for guiding the eye. By analysing how pre-formation probability varies with these parameters,

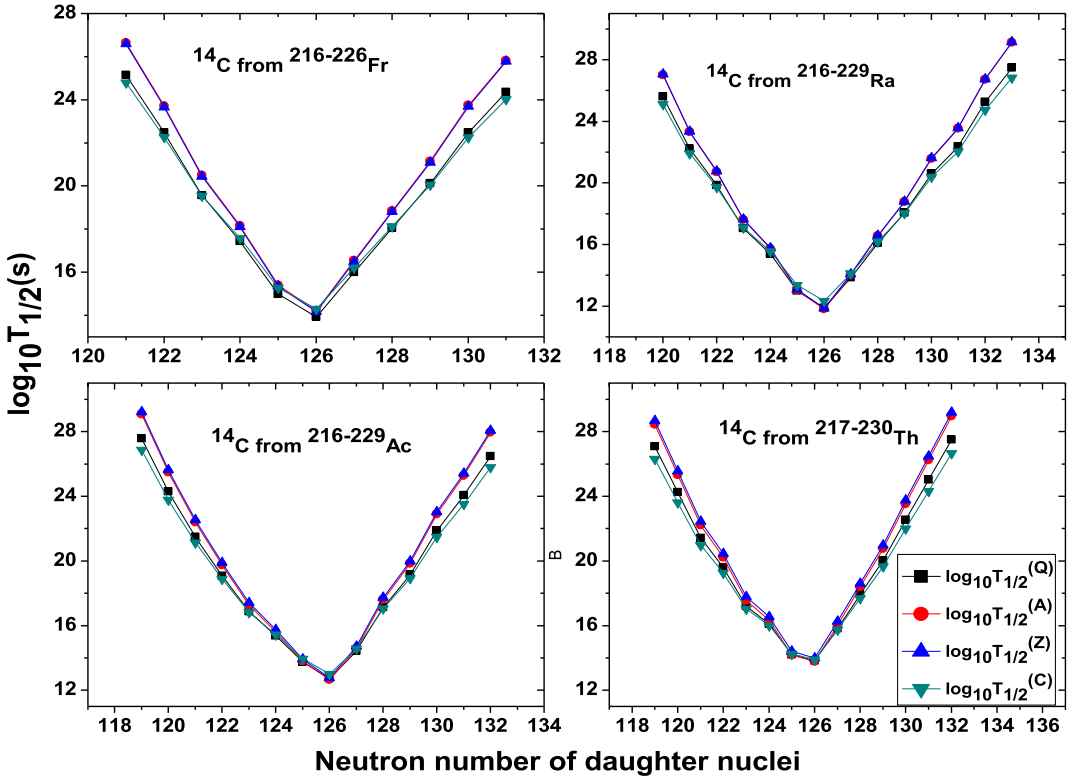

Figure 2. The variation of logarithm of half-life with neutron number of the daughter nucleus for the emission of ^{14}C cluster from various parent nuclei like $^{216-226}$Fr, $^{216-229}$Ra, $^{216-229}$Ac and $^{217-230}$Th.

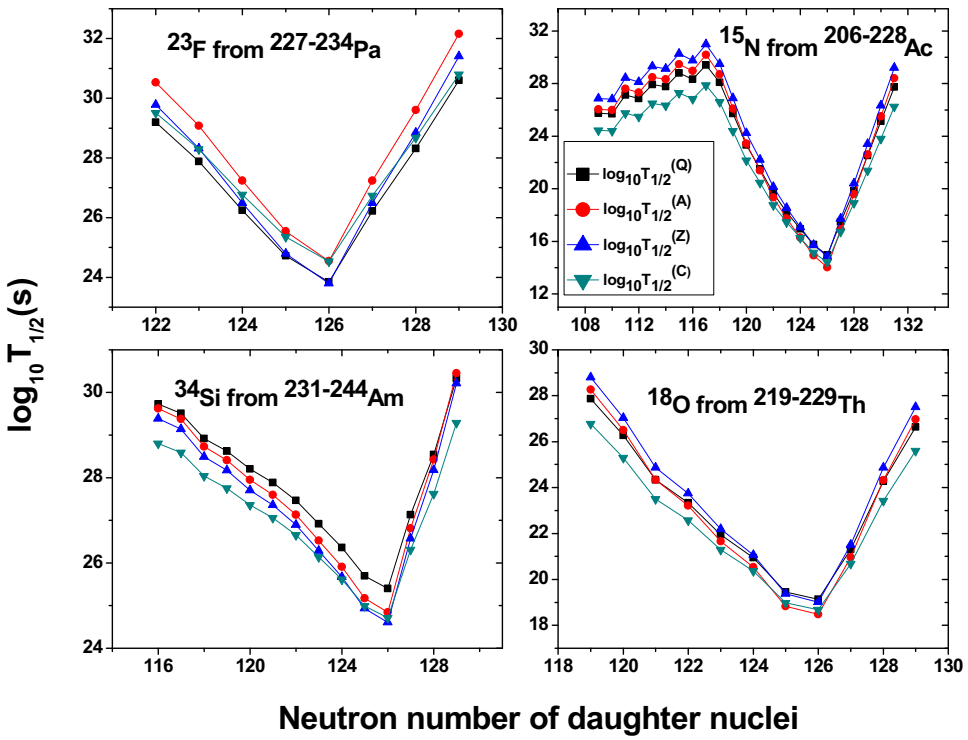

Figure 3. The variation of logarithm of half-lives of cluster emission of ^{23}F from $^{227-234}$Pa, ^{15}N from $^{206-228}$Ac, ^{34}Si from $^{231-244}$Am and ^{18}O from $^{219-229}$Th with neutron number of the daughter nuclei.

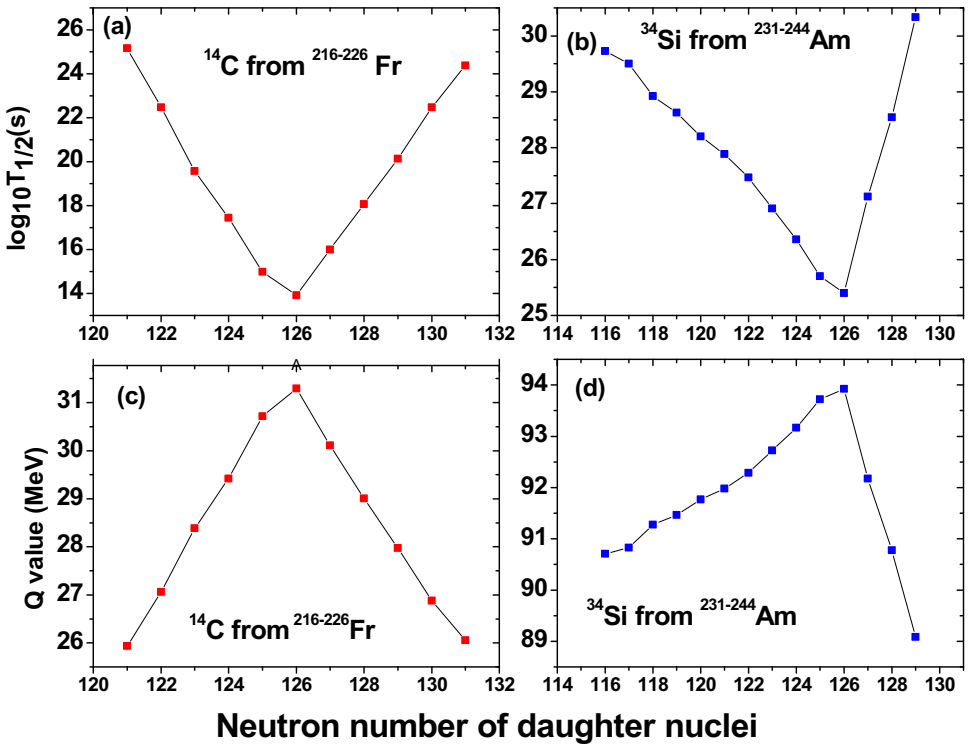

Figure 4. The variation of half-life and Q value with the neutron number of the daughter nucleus for ^{14}C from $^{216-228}$Fr and ^{34}Si from $^{231-244}$Am.

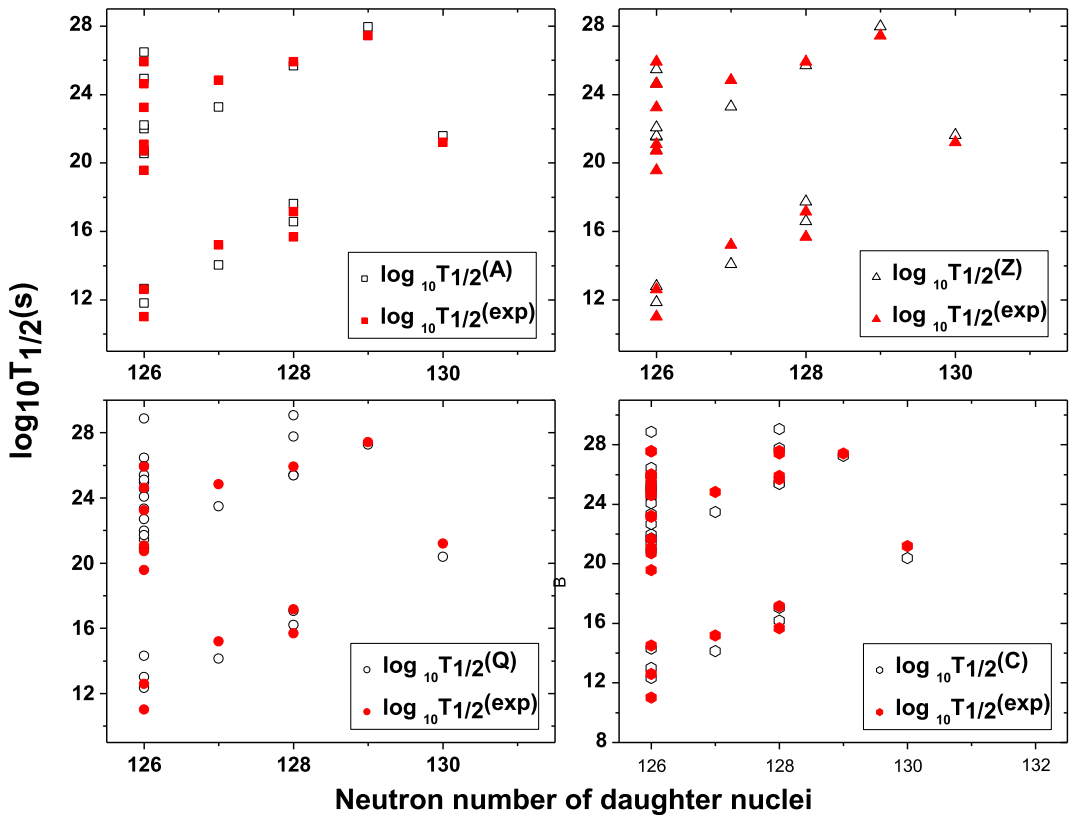

Figure 5. The variation of theoretical half-lives and experimental data.

Table 2. Half-lives of ^{18,20,22}O cluster emission from various isotopes of Ra, Th and U using four types of pre-formation factors.

Cluster reaction	Q_c (MeV)	$\log_{10}[T_{1/2}(s)]$				
		$T_{1/2}^{(Q)}$	$T_{1/2}^{(A)}$	$T_{1/2}^{(Z)}$	$T_{1/2}^{(C)}$	Expt.
^{223}Ra → ^{20}O + ^{203}Hg	38.706	29.79	31.59	30.86	30.05	
^{224}Ra → ^{20}O + ^{204}Hg	39.720	27.77	29.36	28.62	28.16	
^{225}Ra → ^{20}O + ^{205}Hg	40.485	26.29	27.72	26.98	26.77	
^{226}Ra → ^{20}O + ^{206}Hg	40.818	25.62	26.99	26.25	26.15	
^{227}Ra → ^{20}O + ^{207}Hg	39.869	27.30	28.86	28.13	27.71	
^{228}Ra → ^{20}O + ^{208}Hg	38.414	30.06	31.92	31.19	30.28	
^{219}Th → ^{18}O + ^{201}Pb	40.524	27.86	28.26	28.80	26.78	
^{220}Th → ^{18}O + ^{202}Pb	41.393	26.28	26.50	27.04	25.30	
^{221}Th → ^{18}O + ^{203}Pb	42.510	24.34	24.33	24.88	23.51	
^{222}Th → ^{18}O + ^{204}Pb	43.096	23.33	23.21	23.75	22.57	
^{223}Th → ^{18}O + ^{205}Pb	43.939	21.95	21.66	22.20	21.29	
^{224}Th → ^{18}O + ^{206}Pb	44.562	20.95	20.53	21.07	20.36	
^{225}Th → ^{18}O + ^{207}Pb	45.545	19.45	18.83	19.37	18.98	
^{226}Th → ^{18}O + ^{208}Pb	45.729	19.12	18.47	19.01	18.68	>15.30
^{227}Th → ^{18}O + ^{209}Pb	44.202	21.31	20.96	21.50	20.68	
^{228}Th → ^{18}O + ^{210}Pb	42.282	24.28	24.32	24.86	23.42	
^{229}Th → ^{18}O + ^{211}Pb	40.861	26.64	26.97	27.51	25.60	
^{224}Th → ^{20}O + ^{204}Pb	41.308	27.44	28.70	28.22	27.57	
^{225}Th → ^{20}O + ^{205}Pb	42.284	25.64	26.71	26.22	25.89	
^{226}Th → ^{20}O + ^{206}Pb	43.187	24.04	24.92	24.44	24.40	
^{227}Th → ^{20}O + ^{207}Pb	44.461	21.91	22.53	22.05	22.42	
^{228}Th → ^{20}O + ^{208}Pb	44.723	21.43	22.00	21.52	21.98	20.72
^{229}Th → ^{20}O + ^{209}Pb	43.404	23.49	24.33	23.84	23.88	
^{230}Th → ^{20}O + ^{210}Pb	41.795	26.19	27.35	26.87	26.37	
^{231}Th → ^{20}O + ^{211}Pb	40.513	28.46	29.89	29.41	28.49	
^{227}Th → ^{22}O + ^{205}Pb	40.295	30.35	32.85	31.34	31.46	
^{228}Th → ^{22}O + ^{206}Pb	41.277	28.38	30.67	29.16	29.61	
^{229}Th → ^{22}O + ^{207}Pb	42.758	25.58	27.58	26.07	27.00	
^{230}Th → ^{22}O + ^{208}Pb	43.331	24.51	26.39	24.88	26.00	
^{231}Th → ^{22}O + ^{209}Pb	42.151	26.55	28.67	27.16	27.89	
^{232}Th → ^{22}O + ^{210}Pb	40.895	28.85	31.23	29.72	30.04	
^{233}Th → ^{22}O + ^{211}Pb	39.945	30.67	33.24	31.73	31.74	
^{226}U → ^{20}O + ^{206}Po	41.722	29.13	30.31	30.08	28.85	
^{227}U → ^{20}O + ^{207}Po	42.395	27.85	28.89	28.66	27.65	
^{228}U → ^{20}O + ^{208}Po	42.895	26.90	27.84	27.61	26.77	
^{229}U → ^{20}O + ^{209}Po	43.781	25.32	26.08	25.85	25.29	
^{230}U → ^{20}O + ^{210}Po	43.772	25.27	26.04	25.80	25.24	
^{231}U → ^{20}O + ^{211}Po	42.442	27.51	28.54	28.31	27.32	
^{232}U → ^{20}O + ^{212}Po	41.183	29.75	31.04	30.80	29.40	

three main formulae are suggested by our group [46,48] as follows:

- Pre-formation probability may not be the same for alpha and other heavy clusters. It varies with the size of the emitted cluster as

$$P_c = 10^{aA_c+b}, \tag{16}$$

where A_c is the mass number of the cluster, and parameters $a = -0.51325$ and $b = 2.80787$.

- Pre-formation factor also changes with the daughter nuclei and when a different cluster is emitted from the same parent, the relation connecting the product of proton number of the clusterand the daughter

Table 3. Half-lives of ^{22,24,26}Ne cluster emission from various isotopes of Th, Pa and U using four types of pre-formation factors.

Cluster reaction	Q_c (MeV)	$\log_{10}[T_{1/2}(s)]$				
		$T_{1/2}^{(Q)}$	$T_{1/2}^{(A)}$	$T_{1/2}^{(Z)}$	$T_{1/2}^{(C)}$	Expt.
^{223}Th $\rightarrow$ ^{24}Ne + ^{199}Hg	54.884	29.46	30.12	29.82	29.27	
^{224}Th $\rightarrow$ ^{24}Ne + ^{200}Hg	55.449	28.54	29.09	28.79	28.41	
^{225}Th $\rightarrow$ ^{24}Ne + ^{201}Hg	55.924	27.77	28.23	27.93	27.69	
^{226}Th $\rightarrow$ ^{24}Ne + ^{202}Hg	56.495	26.87	27.22	26.93	26.85	
^{227}Th $\rightarrow$ ^{24}Ne + ^{203}Hg	57.026	26.04	26.30	26.00	26.08	
^{228}Th $\rightarrow$ ^{24}Ne + ^{204}Hg	57.413	25.43	25.62	25.32	25.51	
^{229}Th $\rightarrow$ ^{24}Ne + ^{205}Hg	57.825	24.79	24.90	24.60	24.92	
^{230}Th $\rightarrow$ ^{24}Ne + ^{206}Hg	57.760	24.81	24.93	24.63	24.93	24.61
^{231}Th $\rightarrow$ ^{24}Ne + ^{207}Hg	56.255	26.85	27.25	26.95	26.81	
^{232}Th $\rightarrow$ ^{24}Ne + ^{208}Hg	54.668	29.13	29.82	29.52	28.91	>29.20
^{229}Th $\rightarrow$ ^{26}Ne + ^{203}Hg	54.374	30.63	32.41	31.08	31.49	
^{230}Th $\rightarrow$ ^{26}Ne + ^{204}Hg	55.072	29.49	31.14	29.81	30.43	
^{231}Th $\rightarrow$ ^{26}Ne + ^{205}Hg	55.623	28.53	30.07	28.75	29.53	
^{232}Th $\rightarrow$ ^{26}Ne + ^{206}Hg	55.912	28.02	29.51	28.18	29.05	>29.20
^{233}Th $\rightarrow$ ^{26}Ne + ^{207}Hg	54.738	29.76	31.47	30.14	30.66	
^{222}Pa $\rightarrow$ ^{24}Ne + ^{198}Tl	55.641	29.84	30.35	30.21	29.44	
^{223}Pa $\rightarrow$ ^{24}Ne + ^{199}Tl	56.331	28.74	29.12	28.98	28.42	
^{224}Pa $\rightarrow$ ^{24}Ne + ^{200}Tl	56.861	27.89	28.18	28.04	27.63	
^{225}Pa $\rightarrow$ ^{24}Ne + ^{201}Tl	57.473	26.95	27.12	26.98	26.75	
^{226}Pa $\rightarrow$ ^{24}Ne + ^{202}Tl	57.965	26.19	26.27	26.13	26.04	
^{227}Pa $\rightarrow$ ^{24}Ne + ^{203}Tl	58.544	25.32	25.30	25.15	25.24	
^{228}Pa $\rightarrow$ ^{24}Ne + ^{204}Tl	59.222	24.34	24.19	24.05	24.33	
^{229}Pa $\rightarrow$ ^{24}Ne + ^{205}Tl	59.670	23.67	23.45	23.30	23.71	
^{230}Pa $\rightarrow$ ^{24}Ne + ^{206}Tl	60.379	22.68	22.33	22.18	22.79	
^{231}Pa $\rightarrow$ ^{24}Ne + ^{207}Tl	60.410	22.57	22.21	22.07	22.69	23.23
^{232}Pa $\rightarrow$ ^{24}Ne + ^{208}Tl	58.649	24.81	24.77	24.63	24.74	
^{233}Pa $\rightarrow$ ^{24}Ne + ^{209}Tl	57.086	26.91	27.16	27.01	26.67	
^{234}Pa $\rightarrow$ ^{24}Ne + ^{210}Tl	55.538	29.10	29.64	29.49	28.69	
^{235}Pa $\rightarrow$ ^{24}Ne + ^{211}Tl	54.321	30.90	31.66	31.51	30.35	
^{236}Pa $\rightarrow$ ^{24}Ne + ^{212}Tl	52.836	33.21	34.25	34.11	32.50	
^{220}U $\rightarrow$ ^{22}Ne + ^{198}Pb	57.022	28.50	27.73	28.77	26.85	
^{221}U $\rightarrow$ ^{22}Ne + ^{199}Pb	57.777	27.38	26.48	27.51	25.82	
^{222}U $\rightarrow$ ^{22}Ne + ^{200}Pb	58.546	26.28	25.23	26.27	24.79	
^{223}U $\rightarrow$ ^{22}Ne + ^{201}Pb	59.136	25.43	24.27	25.31	24.01	
^{224}U $\rightarrow$ ^{22}Ne + ^{202}Pb	59.688	24.64	23.39	24.42	23.28	
^{225}U $\rightarrow$ ^{22}Ne + ^{203}Pb	60.192	23.93	22.58	23.62	22.62	
^{226}U $\rightarrow$ ^{22}Ne + ^{204}Pb	60.464	23.52	22.12	23.16	22.24	
^{227}U $\rightarrow$ ^{22}Ne + ^{205}Pb	60.840	22.98	21.52	22.56	21.74	
^{228}U $\rightarrow$ ^{22}Ne + ^{206}Pb	61.032	22.67	21.18	22.21	21.46	
^{229}U $\rightarrow$ ^{22}Ne + ^{207}Pb	61.688	21.81	20.19	21.23	20.66	
^{230}U $\rightarrow$ ^{22}Ne + ^{208}Pb	61.388	22.10	20.54	21.57	20.92	19.57
^{231}U $\rightarrow$ ^{22}Ne + ^{209}Pb	59.445	24.45	23.24	24.27	23.06	
^{232}U $\rightarrow$ ^{22}Ne + ^{210}Pb	57.363	27.14	26.31	27.35	25.54	
^{223}U $\rightarrow$ ^{24}Ne + ^{199}Pb	57.024	29.14	29.40	29.41	28.61	
^{224}U $\rightarrow$ ^{24}Ne + ^{200}Pb	57.925	27.77	27.87	27.88	27.34	
^{225}U $\rightarrow$ ^{24}Ne + ^{201}Pb	58.603	26.75	26.72	26.73	26.39	

Table 3. *Continued.*

Cluster reaction	Q_c (MeV)	$\log_{10}[T_{1/2}(s)]$				
		$T_{1/2}^{(Q)}$	$T_{1/2}^{(A)}$	$T_{1/2}^{(Z)}$	$T_{1/2}^{(C)}$	Expt.
$^{226}U \rightarrow {}^{24}Ne + {}^{202}Pb$	59.222	25.83	25.69	25.70	25.53	
$^{227}U \rightarrow {}^{24}Ne + {}^{203}Pb$	59.784	25.01	24.76	24.77	24.77	
$^{228}U \rightarrow {}^{24}Ne + {}^{204}Pb$	60.284	24.27	23.94	23.95	24.09	
$^{229}U \rightarrow {}^{24}Ne + {}^{205}Pb$	60.933	23.36	22.91	22.92	23.24	
$^{230}U \rightarrow {}^{24}Ne + {}^{206}Pb$	61.352	22.76	22.23	22.24	22.68	
$^{231}U \rightarrow {}^{24}Ne + {}^{207}Pb$	62.210	21.62	20.93	20.94	21.63	
$^{232}U \rightarrow {}^{24}Ne + {}^{208}Pb$	62.310	21.42	20.72	20.73	21.44	21.08
$^{233}U \rightarrow {}^{24}Ne + {}^{209}Pb$	60.485	23.65	23.27	23.28	23.48	24.83
$^{234}U \rightarrow {}^{24}Ne + {}^{210}Pb$	58.825	25.79	25.71	25.72	25.44	25.92
$^{235}U \rightarrow {}^{24}Ne + {}^{211}Pb$	57.363	27.76	27.96	27.97	27.26	27.42
$^{236}U \rightarrow {}^{24}Ne + {}^{212}Pb$	55.945	29.77	30.23	30.24	29.12	>25.9
$^{230}U \rightarrow {}^{26}Ne + {}^{204}Pb$	56.244	30.58	32.01	30.99	31.07	
$^{231}U \rightarrow {}^{26}Ne + {}^{205}Pb$	57.095	29.20	30.47	29.46	29.79	
$^{232}U \rightarrow {}^{26}Ne + {}^{206}Pb$	57.914	27.91	29.03	28.02	28.59	
$^{233}U \rightarrow {}^{26}Ne + {}^{207}Pb$	58.890	26.43	27.37	26.36	27.21	
$^{234}U \rightarrow {}^{26}Ne + {}^{208}Pb$	59.413	25.62	26.47	25.45	26.46	25.92
$^{235}U \rightarrow {}^{26}Ne + {}^{209}Pb$	58.052	27.49	28.58	27.57	28.18	
$^{236}U \rightarrow {}^{26}Ne + {}^{210}Pb$	56.692	29.44	30.79	29.77	29.98	>25.90

nuclei is given by

$$P_c = 10^{aZ_cZ_d+b}, \tag{17}$$

where Z_c and Z_d are the atomic numbers of the cluster and the daughter nuclei, and parameters

$a = -0.01555$ and $b = 3.22940$.

- Q value released in a reaction is different for the same cluster ejected from different parent and dependence of pre-formation probability on Q value is

$$P_c = 10^{aQ+bQ^2+c}, \tag{18}$$

where Q is the energy released, parameters a, b and c are given by $a = -0.25736$, $b = 6.37291 \times 10^{-4}$ and $c = 3.35106$.

- As the dependence of pre-formation factor on the three parameters like cluster size, Q value and product of proton number of the cluster and the daughter nuclei is evident, we deduce an expression for pre-formation factor containing all three parameters together in an expression as follows:

$$P_c = 10^{aA_c+bZ_cZ_d+cQ+dQ^2+e}, \tag{19}$$

where a=− 0.5559, b=0.028716, c=− 0.4233358, d=0.001143 and e=1.490754.

3. Results and discussion

Radioactive decay of clusters such as C, N, O, F, Ne, Mg, Si emitted from the nuclei in trans-lead region is examined using MGLDM with the inclusion of four types of pre-formation probabilities. MGLDM is a theoretical method in which GLDM is revised by considering proximity 77 potential [48] as the potential barrier through which cluster tunnel before being emitted. As already stated, four pre-formation factors depend on Q value, cluster size, product of proton number of the cluster and the daughter and a pre-formation factor containing all the three quantities together. Half-lives calculated using these pre-formation factors are represented as $T_{1/2}^{(Q)}$, $T_{1/2}^{(A)}$, $T_{1/2}^{(Z)}$ and $T_{1/2}^{(C)}$ for the combined pre-formation factor.

Theoretically predicted half-lives are shown in tables 1–6. Half-lives determined using these four formulae are listed in a separate column. Table 1 represents the emission of ^{14}C cluster from various isotopes of $^{216-226}$Fr, $^{216-229}$Ra, $^{216-229}$Ac and $^{217-230}$Th. Tables 2–6 show the emission of ^{18,20,22}O from various isotopes of Ra, Th, U; ^{22,24,26}Ne from various isotopes of Th, Pa, U; ^{28,30}Mg from various isotopes of U, Np, Pu; ^{32,34}Si from various isotopes of Pu, Am, Cm; emission of odd clusters ^{15}N, ^{23}F, ^{25}Ne, ^{29}Mg from various isotopes of Ac, Pa, U respectively. The Q values for each decay event are obtained by using the equation, $Q = \Delta M_p - (\Delta M_d + \Delta M_c)$ where ΔM_p, ΔM_d and

Table 4. Half-lives of ^{28,30}Mg cluster emission from various isotopes of U, Np and Pu using four types of pre-formation factors.

Cluster reaction	Q_c (MeV)	$\log_{10}[T_{1/2}(s)]$				
		$T_{1/2}^{(Q)}$	$T_{1/2}^{(A)}$	$T_{1/2}^{(Z)}$	$T_{1/2}^{(C)}$	Expt.
$^{223}U \rightarrow {}^{28}Mg + {}^{195}Hg$	71.872	29.64	29.35	29.49	28.81	
$^{224}U \rightarrow {}^{28}Mg + {}^{196}Hg$	72.567	28.70	28.30	28.43	27.93	
$^{225}U \rightarrow {}^{28}Mg + {}^{197}Hg$	72.939	28.16	27.70	27.83	27.43	
$^{226}U \rightarrow {}^{28}Mg + {}^{198}Hg$	73.302	27.64	27.12	27.25	26.94	
$^{227}U \rightarrow {}^{28}Mg + {}^{199}Hg$	73.610	27.19	26.61	26.75	26.52	
$^{228}U \rightarrow {}^{28}Mg + {}^{200}Hg$	73.744	26.95	26.35	26.49	26.29	
$^{229}U \rightarrow {}^{28}Mg + {}^{201}Hg$	73.892	26.69	26.07	26.20	26.04	
$^{230}U \rightarrow {}^{28}Mg + {}^{202}Hg$	73.979	26.51	25.87	26.00	25.86	
$^{231}U \rightarrow {}^{28}Mg + {}^{203}Hg$	74.094	26.29	25.63	25.77	25.66	
$^{232}U \rightarrow {}^{28}Mg + {}^{204}Hg$	74.318	25.95	25.25	25.39	25.33	>22.26
$^{233}U \rightarrow {}^{28}Mg + {}^{205}Hg$	74.226	25.97	25.29	25.43	25.35	>27.59
$^{234}U \rightarrow {}^{28}Mg + {}^{206}Hg$	74.110	26.03	25.37	25.50	25.40	27.54
$^{235}U \rightarrow {}^{28}Mg + {}^{207}Hg$	72.425	27.96	27.58	27.71	27.18	>28.10
$^{236}U \rightarrow {}^{28}Mg + {}^{208}Hg$	70.733	30.00	29.90	30.03	29.05	27.58
$^{232}U \rightarrow {}^{30}Mg + {}^{202}Hg$	70.839	30.74	31.64	30.75	30.92	
$^{233}U \rightarrow {}^{30}Mg + {}^{203}Hg$	71.073	30.35	31.21	30.32	30.55	
$^{234}U \rightarrow {}^{30}Mg + {}^{204}Hg$	71.719	29.42	30.18	29.29	29.68	
$^{235}U \rightarrow {}^{30}Mg + {}^{205}Hg$	72.091	28.86	29.56	28.67	29.16	
$^{236}U \rightarrow {}^{30}Mg + {}^{206}Hg$	72.275	28.55	29.22	28.32	28.86	27.58
$^{237}U \rightarrow {}^{30}Mg + {}^{207}Hg$	70.761	30.42	31.35	30.45	30.60	
$^{232}Np \rightarrow {}^{30}Mg + {}^{202}Tl$	72.224	30.51	31.18	30.48	30.47	
$^{233}Np \rightarrow {}^{30}Mg + {}^{203}Tl$	72.595	29.94	30.56	29.85	29.94	
$^{234}Np \rightarrow {}^{30}Mg + {}^{204}Tl$	73.185	29.11	29.63	28.92	29.16	
$^{235}Np \rightarrow {}^{30}Mg + {}^{205}Tl$	73.748	28.32	28.75	28.04	28.43	
$^{236}Np \rightarrow {}^{30}Mg + {}^{206}Tl$	74.517	27.29	27.59	26.89	27.47	
$^{237}Np \rightarrow {}^{30}Mg + {}^{207}Tl$	74.790	26.88	27.14	26.43	27.08	>26.93
$^{238}Np \rightarrow {}^{30}Mg + {}^{208}Tl$	73.089	28.90	29.43	28.73	28.94	
$^{239}Np \rightarrow {}^{30}Mg + {}^{209}Tl$	71.840	30.42	31.16	30.46	30.35	
$^{228}Pu \rightarrow {}^{28}Mg + {}^{200}Pb$	77.357	25.72	24.54	25.05	24.69	
$^{229}Pu \rightarrow {}^{28}Mg + {}^{201}Pb$	77.690	25.26	24.03	24.54	24.27	
$^{230}Pu \rightarrow {}^{28}Mg + {}^{202}Pb$	77.894	24.96	23.69	24.20	23.97	
$^{231}Pu \rightarrow {}^{28}Mg + {}^{203}Pb$	78.115	24.63	23.33	23.84	23.67	
$^{232}Pu \rightarrow {}^{28}Mg + {}^{204}Pb$	78.492	24.14	22.77	23.28	23.21	
$^{233}Pu \rightarrow {}^{28}Mg + {}^{205}Pb$	78.839	23.68	22.26	22.77	22.78	
$^{234}Pu \rightarrow {}^{28}Mg + {}^{206}Pb$	79.154	23.26	21.79	22.30	22.39	
$^{235}Pu \rightarrow {}^{28}Mg + {}^{207}Pb$	79.653	22.65	21.11	21.61	21.82	
$^{236}Pu \rightarrow {}^{28}Mg + {}^{208}Pb$	79.669	22.55	21.01	21.51	21.72	21.67
$^{237}Pu \rightarrow {}^{28}Mg + {}^{209}Pb$	77.725	24.56	23.33	23.83	23.57	
$^{238}Pu \rightarrow {}^{28}Mg + {}^{210}Pb$	75.911	26.53	25.58	26.09	25.38	25.70
$^{239}Pu \rightarrow {}^{28}Mg + {}^{211}Pb$	74.100	28.59	27.94	28.45	27.27	
$^{232}Pu \rightarrow {}^{30}Mg + {}^{202}Pb$	73.188	30.83	31.34	30.83	30.53	
$^{233}Pu \rightarrow {}^{30}Mg + {}^{203}Pb$	73.721	30.06	30.49	29.97	29.82	
$^{234}Pu \rightarrow {}^{30}Mg + {}^{204}Pb$	74.344	29.19	29.52	29.01	29.01	
$^{235}Pu \rightarrow {}^{30}Mg + {}^{205}Pb$	74.836	28.50	28.75	28.23	28.36	
$^{236}Pu \rightarrow {}^{30}Mg + {}^{206}Pb$	75.571	27.52	27.66	27.14	27.45	
$^{237}Pu \rightarrow {}^{30}Mg + {}^{207}Pb$	76.428	26.42	26.41	25.89	26.42	
$^{238}Pu \rightarrow {}^{30}Mg + {}^{208}Pb$	76.796	25.90	25.84	25.32	25.94	25.70
$^{239}Pu \rightarrow {}^{30}Mg + {}^{209}Pb$	75.087	27.86	28.07	27.55	27.74	
$^{240}Pu \rightarrow {}^{30}Mg + {}^{210}Pb$	73.738	29.45	29.88	29.36	29.21	

Table 5. Half-lives of ^{32,34}Si cluster emission from various isotopes of Pu, Am and Cm using four types of pre-formation factors.

Cluster reaction	Q_c (MeV)	$\log_{10}[T_{1/2}(\mathrm{s})]$				
		$T_{1/2}^{(Q)}$	$T_{1/2}^{(A)}$	$T_{1/2}^{(Z)}$	$T_{1/2}^{(C)}$	Expt.
$^{228}\mathrm{Pu} \rightarrow {}^{32}\mathrm{Si} + {}^{196}\mathrm{Hg}$	91.991	26.79	25.47	26.04	25.25	
$^{229}\mathrm{Pu} \rightarrow {}^{32}\mathrm{Si} + {}^{197}\mathrm{Hg}$	92.018	26.67	25.35	25.92	25.13	
$^{230}\mathrm{Pu} \rightarrow {}^{32}\mathrm{Si} + {}^{198}\mathrm{Hg}$	91.966	26.63	25.32	25.89	25.09	
$^{231}\mathrm{Pu} \rightarrow {}^{32}\mathrm{Si} + {}^{199}\mathrm{Hg}$	91.933	26.57	25.26	25.83	25.03	
$^{232}\mathrm{Pu} \rightarrow {}^{32}\mathrm{Si} + {}^{200}\mathrm{Hg}$	91.944	26.46	25.16	25.73	24.92	
$^{233}\mathrm{Pu} \rightarrow {}^{32}\mathrm{Si} + {}^{201}\mathrm{Hg}$	91.790	26.53	25.24	25.81	24.98	
$^{234}\mathrm{Pu} \rightarrow {}^{32}\mathrm{Si} + {}^{202}\mathrm{Hg}$	91.773	26.46	25.17	25.74	24.90	
$^{235}\mathrm{Pu} \rightarrow {}^{32}\mathrm{Si} + {}^{203}\mathrm{Hg}$	91.529	26.61	25.36	25.93	25.04	
$^{236}\mathrm{Pu} \rightarrow {}^{32}\mathrm{Si} + {}^{204}\mathrm{Hg}$	91.669	26.38	25.11	25.68	24.82	
$^{237}\mathrm{Pu} \rightarrow {}^{32}\mathrm{Si} + {}^{205}\mathrm{Hg}$	91.457	26.51	25.27	25.84	24.93	
$^{238}\mathrm{Pu} \rightarrow {}^{32}\mathrm{Si} + {}^{206}\mathrm{Hg}$	91.187	26.70	25.50	26.07	25.10	25.27
$^{239}\mathrm{Pu} \rightarrow {}^{32}\mathrm{Si} + {}^{207}\mathrm{Hg}$	89.153	28.76	27.84	28.41	27.01	
$^{230}\mathrm{Pu} \rightarrow {}^{34}\mathrm{Si} + {}^{196}\mathrm{Hg}$	88.717	30.38	30.56	30.10	29.71	
$^{231}\mathrm{Pu} \rightarrow {}^{34}\mathrm{Si} + {}^{197}\mathrm{Hg}$	88.806	30.19	30.35	29.89	29.52	
$^{232}\mathrm{Pu} \rightarrow {}^{34}\mathrm{Si} + {}^{198}\mathrm{Hg}$	89.274	29.57	29.67	29.21	28.94	
$^{233}\mathrm{Pu} \rightarrow {}^{34}\mathrm{Si} + {}^{199}\mathrm{Hg}$	89.553	29.17	29.23	28.77	28.56	
$^{234}\mathrm{Pu} \rightarrow {}^{34}\mathrm{Si} + {}^{200}\mathrm{Hg}$	89.810	28.79	28.81	28.36	28.21	
$^{235}\mathrm{Pu} \rightarrow {}^{34}\mathrm{Si} + {}^{201}\mathrm{Hg}$	89.802	28.71	28.73	28.27	28.12	
$^{236}\mathrm{Pu} \rightarrow {}^{34}\mathrm{Si} + {}^{202}\mathrm{Hg}$	90.204	28.18	28.14	27.69	27.62	
$^{237}\mathrm{Pu} \rightarrow {}^{34}\mathrm{Si} + {}^{203}\mathrm{Hg}$	90.318	27.96	27.91	27.45	27.41	
$^{238}\mathrm{Pu} \rightarrow {}^{34}\mathrm{Si} + {}^{204}\mathrm{Hg}$	90.810	27.34	27.22	26.76	26.83	
$^{239}\mathrm{Pu} \rightarrow {}^{34}\mathrm{Si} + {}^{205}\mathrm{Hg}$	90.833	27.23	27.10	26.64	26.71	
$^{240}\mathrm{Pu} \rightarrow {}^{34}\mathrm{Si} + {}^{206}\mathrm{Hg}$	91.028	26.93	26.77	26.32	26.43	>25.52
$^{241}\mathrm{Pu} \rightarrow {}^{34}\mathrm{Si} + {}^{207}\mathrm{Hg}$	89.399	28.60	28.68	28.23	27.99	
$^{242}\mathrm{Pu} \rightarrow {}^{34}\mathrm{Si} + {}^{208}\mathrm{Hg}$	87.944	30.14	30.43	29.98	29.42	
$^{231}\mathrm{Am} \rightarrow {}^{34}\mathrm{Si} + {}^{197}\mathrm{Tl}$	90.709	29.73	29.62	29.38	28.81	
$^{232}\mathrm{Am} \rightarrow {}^{34}\mathrm{Si} + {}^{198}\mathrm{Tl}$	90.826	29.50	29.38	29.14	28.59	
$^{233}\mathrm{Am} \rightarrow {}^{34}\mathrm{Si} + {}^{199}\mathrm{Tl}$	91.276	28.92	28.73	28.49	28.04	
$^{234}\mathrm{Am} \rightarrow {}^{34}\mathrm{Si} + {}^{200}\mathrm{Tl}$	91.464	28.62	28.41	28.17	27.76	
$^{235}\mathrm{Am} \rightarrow {}^{34}\mathrm{Si} + {}^{201}\mathrm{Tl}$	91.768	28.20	27.95	27.71	27.36	
$^{236}\mathrm{Am} \rightarrow {}^{34}\mathrm{Si} + {}^{202}\mathrm{Tl}$	91.977	27.89	27.60	27.36	27.06	
$^{237}\mathrm{Am} \rightarrow {}^{34}\mathrm{Si} + {}^{203}\mathrm{Tl}$	92.288	27.46	27.14	26.90	26.66	
$^{238}\mathrm{Am} \rightarrow {}^{34}\mathrm{Si} + {}^{204}\mathrm{Tl}$	92.723	26.91	26.52	26.29	26.14	
$^{239}\mathrm{Am} \rightarrow {}^{34}\mathrm{Si} + {}^{205}\mathrm{Tl}$	93.168	26.36	25.91	25.67	25.62	
$^{240}\mathrm{Am} \rightarrow {}^{34}\mathrm{Si} + {}^{206}\mathrm{Tl}$	93.720	25.70	25.17	24.93	25.00	
$^{241}\mathrm{Am} \rightarrow {}^{34}\mathrm{Si} + {}^{207}\mathrm{Tl}$	93.925	25.40	24.84	24.60	24.71	>24.41
$^{242}\mathrm{Am} \rightarrow {}^{34}\mathrm{Si} + {}^{208}\mathrm{Tl}$	92.175	27.13	26.81	26.58	26.31	
$^{243}\mathrm{Am} \rightarrow {}^{34}\mathrm{Si} + {}^{209}\mathrm{Tl}$	90.777	28.54	28.42	28.18	27.62	
$^{244}\mathrm{Am} \rightarrow {}^{34}\mathrm{Si} + {}^{210}\mathrm{Tl}$	89.083	30.33	30.45	30.22	29.29	
$^{233}\mathrm{Cm} \rightarrow {}^{34}\mathrm{Si} + {}^{199}\mathrm{Pb}$	92.479	29.24	28.89	28.86	28.05	
$^{234}\mathrm{Cm} \rightarrow {}^{34}\mathrm{Si} + {}^{200}\mathrm{Pb}$	92.933	28.66	28.24	28.22	27.50	
$^{235}\mathrm{Cm} \rightarrow {}^{34}\mathrm{Si} + {}^{201}\mathrm{Pb}$	93.258	28.22	27.76	27.74	27.08	
$^{236}\mathrm{Cm} \rightarrow {}^{34}\mathrm{Si} + {}^{202}\mathrm{Pb}$	93.753	27.61	27.08	27.06	26.51	
$^{237}\mathrm{Cm} \rightarrow {}^{34}\mathrm{Si} + {}^{203}\mathrm{Pb}$	93.994	27.26	26.70	26.68	26.18	
$^{238}\mathrm{Cm} \rightarrow {}^{34}\mathrm{Si} + {}^{204}\mathrm{Pb}$	94.512	26.64	26.00	25.98	25.59	
$^{239}\mathrm{Cm} \rightarrow {}^{34}\mathrm{Si} + {}^{205}\mathrm{Pb}$	94.877	26.17	25.48	25.46	25.15	

Table 5. *Continued.*

Cluster reaction	Q_c (MeV)	$\log_{10}[T_{1/2}(s)]$				
		$T_{1/2}^{(Q)}$	$T_{1/2}^{(A)}$	$T_{1/2}^{(Z)}$	$T_{1/2}^{(C)}$	Expt.
$^{240}Cm \rightarrow {}^{34}Si + {}^{206}Pb$	95.467	25.48	24.71	24.69	24.50	
$^{241}Cm \rightarrow {}^{34}Si + {}^{207}Pb$	96.111	24.74	23.89	23.87	23.81	
$^{242}Cm \rightarrow {}^{34}Si + {}^{208}Pb$	96.509	24.26	23.35	23.33	23.35	23.15
$^{243}Cm \rightarrow {}^{34}Si + {}^{209}Pb$	94.754	25.93	25.26	25.24	24.90	
$^{244}Cm \rightarrow {}^{34}Si + {}^{210}Pb$	93.137	27.52	27.07	27.05	26.37	
$^{245}Cm \rightarrow {}^{34}Si + {}^{211}Pb$	91.455	29.24	29.02	29.00	27.97	

ΔM_c are the mass excesses of the parent, the daughter and the cluster. Excess mass values are obtained from the recent mass table of Audi *et al* [49].

Table 1 lists the emission of ^{14}C from $^{216-226}Fr$, $^{216-229}Ra$, $^{216-229}Ac$ and $^{217-230}Th$. A graph is plotted with values from table 1 with neutron number of the daughter nuclei along the X-axis and logarithm of half-lives in seconds along the Y-axis and is shown in figure 2. Black square in the graph represents half-lives computed using Q-dependent pre-formation factor, red circle, blue triangle and green inverted triangle denote half-lives calculated using cluster size-dependent, product of atomic number of the daughter and the cluster-dependent pre-formation factor and with the combined pre-formation factor respectively. In all the four cases, it is evident that as neutron number of the daughter nucleus increases, logarithm of half-life decreases and reaches a minimum value and then increases. An interesting fact noticed from all these graphs is that minimum point of all graphs corresponds to a value $N = 126$, which is a magic number. Therefore, it is clear that when the neutron number of the daughter nucleus is a magic number, the corresponding half-life will be minimum. Thus, the emission of ^{14}C from different parents proves neutron shell effects with maximum stability and minimum half-life.

Figure 2 verifies neutron shell effect in the case of ^{14}C emission from various parent nuclei. In order to generalise this effect, we plot the same graph with neutron number of the daughter nucleus along the X-axis and logarithm of half-life along the Y-axis for all the values from tables 2–6. Among these, emission of ^{23}F from $^{227-234}Pa$, ^{15}N from $^{206-228}Ac$, ^{34}Si from $^{231-244}Am$ and ^{18}O from $^{219-229}Th$ are shown in figure 2. Figures 2 and 3 look similar with all the curves having a minimum point at $N = 126$. Thus, it is stressed that the maximum stability is attained for processes leading to magic daughter nucleus with minimum half-life.

Again, a graph is drawn showing variation of half-lives corresponding to Q-dependent pre-formation factor and Q value with the neutron number of the daughter nucleus in figure 4. Figure 4a shows how the logarithm of half-life varies with neutron number of the daughter nucleus and figure 4c shows variation of Q value with neutron number of the daughter nuclei in the case of ^{14}C from $^{216-228}Fr$. Figures 4b and 4d show the same variation in the case of ^{34}Si from $^{231-244}Am$. For a particular cluster reaction, both graphs of Q value and half-life are exactly the mirror image of each other. In figure 4a, $N = 126$ is the minimum point of the curve whereas in figure 4c, it is the maximum point of the curve. Hence, both half-life and Q value are inversely proportional and for any cluster emission when Q value increases, the barrier height $(V-Q)$ decreases and can tunnel easily through the potential barrier and hence half-lives decrease. This relation between Q value and half-life and the main role of Q value in determining cluster half-life are clearly pointed out through calculated results.

Figure 5 clearly demonstrates how precisely the predicted half-lives coincide with the experimental data. In the graph, solid circle shows the experimental values from tables 1–6. Empty square, circle, triangle and hexagon denote half-lives using the cluster, size-dependent, Q value-dependent, product of atomic number of the cluster and the daughter-dependent pre-formation factor and with combined pre-formation factor from tables 1–6 whose experimental values are known. From the graph, one can point out that, using MGLDM with different pre-formation factors, experimental values are reproduced with great accuracy. Again from the graph, it is clear that majority of the daughter nuclei in the cluster decay have magic number of neutrons ($N = 126$). Hence, stability of the magic daughter nuclei is stressed here again.

The standard deviation of the present approach is calculated using the equation

$$\sigma = \sqrt{\frac{1}{N}\sum_{i=1}^{N}\left[\left(\log_{10} T_{1/2}^{\text{theor}} - \log_{10} T_{1/2}^{\text{exp}}\right)^2\right]}. \qquad (20)$$

Table 6. The predicted half-lives for the emission of the odd clusters ^{15}N, ^{23}F, ^{25}Ne and ^{29}Mg from various isotopes of Ac, Pa and U. The half-lives are calculated using four types of pre-formation factor.

Cluster reaction	Q_c (MeV)	$\log_{10}[T_{1/2}(s)]$				
		$T_{1/2}^{(Q)}$	$T_{1/2}^{(A)}$	$T_{1/2}^{(Z)}$	$T_{1/2}^{(C)}$	Expt.
^{206}Ac $\rightarrow$ ^{15}N + ^{191}Pb	33.609	25.74	26.05	26.86	24.46	
^{207}Ac $\rightarrow$ ^{15}N + ^{192}Pb	33.605	25.69	26.00	26.81	24.40	
^{208}Ac $\rightarrow$ ^{15}N + ^{193}Pb	32.839	27.14	27.62	28.43	25.76	
^{209}Ac $\rightarrow$ ^{15}N + ^{194}Pb	32.947	26.87	27.32	28.13	25.50	
^{210}Ac $\rightarrow$ ^{15}N + ^{195}Pb	32.397	27.93	28.50	29.31	26.49	
^{211}Ac $\rightarrow$ ^{15}N + ^{196}Pb	32.447	27.76	28.33	29.13	26.33	
^{212}Ac $\rightarrow$ ^{15}N + ^{197}Pb	31.924	28.80	29.48	30.28	27.30	
^{213}Ac $\rightarrow$ ^{15}N + ^{198}Pb	32.121	28.33	28.96	29.76	26.85	
^{214}Ac $\rightarrow$ ^{15}N + ^{199}Pb	31.575	29.43	30.18	30.99	27.88	
^{215}Ac $\rightarrow$ ^{15}N + ^{200}Pb	32.181	28.08	28.70	29.51	26.61	
^{216}Ac $\rightarrow$ ^{15}N + ^{201}Pb	33.314	25.72	26.10	26.90	24.40	
^{217}Ac $\rightarrow$ ^{15}N + ^{202}Pb	34.544	23.32	23.44	24.24	22.16	
^{218}Ac $\rightarrow$ ^{15}N + ^{203}Pb	35.526	21.50	21.41	22.21	20.47	
^{219}Ac $\rightarrow$ ^{15}N + ^{204}Pb	36.578	19.65	19.33	20.14	18.76	
^{220}Ac $\rightarrow$ ^{15}N + ^{205}Pb	37.413	18.24	17.75	18.55	17.45	
^{221}Ac $\rightarrow$ ^{15}N + ^{206}Pb	38.204	16.95	16.29	17.10	16.27	
^{222}Ac $\rightarrow$ ^{15}N + ^{207}Pb	38.972	15.75	14.93	15.73	15.16	
^{223}Ac $\rightarrow$ ^{15}N + ^{208}Pb	39.473	14.96	14.04	14.84	14.44	$>$14.76
^{224}Ac $\rightarrow$ ^{15}N + ^{209}Pb	37.747	17.50	16.93	17.74	16.75	
^{225}Ac $\rightarrow$ ^{15}N + ^{210}Pb	36.264	19.85	19.59	20.40	18.91	
^{226}Ac $\rightarrow$ ^{15}N + ^{211}Pb	34.700	22.54	22.62	23.42	21.40	
^{227}Ac $\rightarrow$ ^{15}N + ^{212}Pb	33.297	25.14	25.52	26.33	23.82	
^{228}Ac $\rightarrow$ ^{15}N + ^{213}Pb	31.997	27.74	28.40	29.21	26.25	
^{227}Pa $\rightarrow$ ^{23}F + ^{204}Pb	48.651	29.19	30.53	29.78	29.52	
^{228}Pa $\rightarrow$ ^{23}F + ^{205}Pb	49.404	27.88	29.07	28.32	28.29	
^{229}Pa $\rightarrow$ ^{23}F + ^{206}Pb	50.393	26.24	27.24	26.49	26.76	
^{230}Pa $\rightarrow$ ^{23}F + ^{207}Pb	51.336	24.72	25.54	24.79	25.36	
^{231}Pa $\rightarrow$ ^{23}F + ^{208}Pb	51.883	23.84	24.55	23.80	24.53	26.02
^{232}Pa $\rightarrow$ ^{23}F + ^{209}Pb	50.272	26.22	27.24	26.49	26.73	
^{233}Pa $\rightarrow$ ^{23}F + ^{210}Pb	48.928	28.32	29.60	28.85	28.67	
^{234}Pa $\rightarrow$ ^{23}F + ^{211}Pb	47.542	30.60	32.15	31.40	30.79	
^{227}U $\rightarrow$ ^{25}Ne + ^{202}Pb	57.022	29.24	30.01	29.51	29.26	
^{228}U $\rightarrow$ ^{25}Ne + ^{203}Pb	56.045	30.63	31.59	31.08	30.55	
^{229}U $\rightarrow$ ^{25}Ne + ^{204}Pb	58.357	27.15	27.68	27.18	27.32	
^{230}U $\rightarrow$ ^{25}Ne + ^{205}Pb	57.421	28.43	29.12	28.62	28.49	
^{231}U $\rightarrow$ ^{25}Ne + ^{206}Pb	59.628	25.24	25.54	25.03	25.54	
^{232}U $\rightarrow$ ^{25}Ne + ^{207}Pb	59.098	25.89	26.28	25.78	26.14	
^{233}U $\rightarrow$ ^{25}Ne + ^{208}Pb	60.704	23.66	23.76	23.26	24.07	24.84
^{234}U $\rightarrow$ ^{25}Ne + ^{209}Pb	57.796	27.59	28.21	27.71	27.69	
^{235}U $\rightarrow$ ^{25}Ne + ^{210}Pb	57.683	27.68	28.33	27.82	27.77	27.42
^{229}U $\rightarrow$ ^{29}Mg + ^{200}Hg	71.317	30.10	30.42	30.04	29.77	
^{230}U $\rightarrow$ ^{29}Mg + ^{201}Hg	69.881	31.90	32.45	32.07	31.43	
^{231}U $\rightarrow$ ^{29}Mg + ^{202}Hg	71.754	29.38	29.62	29.24	29.09	
^{232}U $\rightarrow$ ^{29}Mg + ^{203}Hg	70.482	30.94	31.39	31.01	30.52	
^{233}U $\rightarrow$ ^{29}Mg + ^{204}Hg	72.632	28.11	28.21	27.83	27.90	
^{234}U $\rightarrow$ ^{29}Mg + ^{205}Hg	71.036	30.05	30.41	30.03	29.69	
^{235}U $\rightarrow$ ^{29}Mg + ^{206}Hg	72.468	28.15	28.28	27.90	27.93	$>$ 28.09

Table 7. The comparison of the predicted half-lives for alpha emission from various isotopes with the experimental half-lives using four types pre-formation factors.

Parent nuclei	Daughter nuclei	Q_α (MeV)	$\log_{10}[T_{1/2}(\mathrm{s})]$				
			$T_{1/2}^{(Q)}$	$T_{1/2}^{(A)}$	$T_{1/2}^{(Z)}$	$T_{1/2}^{(C)}$	Expt.
^{215}At	^{211}Bi	8.178	− 5.38	− 4.85	− 4.74	− 4.74	− 4.000
^{215}Rn	^{211}Po	8.839	− 6.69	− 6.31	− 6.18	− 6.00	− 5.638
^{216}Rn	^{212}Po	8.198	− 5.06	− 4.53	− 4.39	− 4.48	− 4.347
^{217}Rn	^{213}Po	7.888	− 4.21	− 3.60	− 3.46	− 3.67	− 3.268
^{218}Rn	^{214}Po	7.262	− 2.28	− 1.52	− 1.38	− 1.84	− 1.456
^{219}Rn	^{215}Po	6.946	− 1.21	− 0.37	− 0.23	− 0.82	0.598
^{220}Rn	^{216}Po	6.405	0.84	1.81	1.95	1.14	1.745
^{222}Rn	^{218}Po	5.591	4.51	5.69	5.83	4.68	5.519
^{216}Fr	^{212}At	9.174	− 7.12	− 6.83	− 6.66	− 6.44	− 6.155
^{217}Fr	^{213}At	8.470	− 5.41	− 4.95	− 4.78	− 4.84	− 4.721
^{218}Fr	^{214}At	8.014	− 4.18	− 3.61	− 3.44	− 3.68	− 3.000
^{219}Fr	^{215}At	7.449	− 2.48	− 1.77	− 1.60	− 2.07	− 1.699
^{220}Fr	^{216}At	6.800	− 0.24	0.63	0.80	0.06	1.438
^{221}Fr	^{217}At	6.457	1.08	2.04	2.21	1.33	2.457
^{217}Ra	^{213}Rn	9.161	− 6.74	− 6.45	− 6.25	− 6.12	− 5.796
^{218}Ra	^{214}Rn	8.546	− 5.24	− 4.80	− 4.60	− 4.72	− 4.599
^{219}Ra	^{215}Rn	8.138	− 4.15	− 3.61	− 3.41	− 3.69	− 2.000
^{220}Ra	^{216}Rn	7.592	− 2.54	− 1.86	− 1.66	− 2.16	− 1.745
^{221}Ra	^{217}Rn	6.880	− 0.11	0.74	0.94	0.15	1.447
^{222}Ra	^{218}Rn	6.678	0.64	1.55	1.75	0.87	1.580
^{223}Ra	^{219}Rn	5.979	3.61	4.69	4.89	3.73	5.995
^{224}Ra	^{220}Rn	5.789	4.51	5.63	5.83	4.59	5.497
^{226}Ra	^{222}Rn	4.871	9.66	11.02	11.22	9.60	10.703
^{217}Ac	^{213}Fr	9.832	− 7.86	− 7.74	− 7.51	− 7.19	− 7.161
^{218}Ac	^{214}Fr	9.374	− 6.88	− 6.64	− 6.41	− 6.28	− 5.967
^{219}Ac	^{215}Fr	8.827	− 5.60	− 5.22	− 4.99	− 5.08	− 4.928
^{220}Ac	^{216}Fr	8.348	− 4.36	− 3.87	− 3.64	− 3.92	− 1.578
^{221}Ac	^{217}Fr	7.780	− 2.73	− 2.10	− 1.86	− 2.38	− 1.284
^{222}Ac	^{218}Fr	7.137	− 0.62	0.17	0.40	− 0.38	0.699
^{223}Ac	^{219}Fr	6.783	0.67	1.55	1.78	0.86	2.100
^{224}Ac	^{220}Fr	6.327	2.52	3.51	3.74	2.63	4.000
^{225}Ac	^{221}Fr	5.935	4.28	5.37	5.60	4.33	5.937
^{226}Ac	^{222}Fr	5.506	6.45	7.65	7.88	6.43	5.024
^{227}Ac	^{223}Fr	5.042	9.12	10.44	10.67	9.03	8.837
^{217}Th	^{213}Ra	9.435	− 6.64	− 6.41	− 6.15	− 6.09	− 3.618
^{219}Th	^{215}Ra	9.511	− 6.84	− 6.64	− 6.38	−6.28	− 5.979
^{220}Th	^{216}Ra	8.953	− 5.55	− 5.21	− 4.94	− 5.08	− 5.013
^{221}Th	^{217}Ra	8.625	− 4.73	− 4.31	− 4.05	− 4.31	− 2.775
^{222}Th	^{218}Ra	8.127	− 3.38	− 2.83	− 2.57	− 3.03	− 2.553
^{223}Th	^{219}Ra	7.567	− 1.67	− 0.99	− 0.73	− 1.42	− 0.222
^{224}Th	^{220}Ra	7.299	− 0.79	− 0.04	0.22	− 0.58	0.017
^{225}Th	^{221}Ra	6.921	0.56	1.40	1.67	0.71	2.720
^{226}Th	^{222}Ra	6.453	2.41	3.38	3.64	2.49	3.263
^{228}Th	^{224}Ra	5.520	6.86	8.05	8.32	6.79	7.780
^{229}Th	^{225}Ra	5.168	8.86	10.15	10.41	8.74	11.398
^{230}Th	^{226}Ra	4.770	11.41	12.80	13.06	11.22	12.376

Table 7. *Continued.*

Parent nuclei	Daughter nuclei	Q_α (MeV)	$\log_{10}[T_{1/2}(s)]$				
			$T_{1/2}^{(Q)}$	$T_{1/2}^{(A)}$	$T_{1/2}^{(Z)}$	$T_{1/2}^{(C)}$	Expt.
^{232}Th	^{228}Ra	4.082	16.72	18.28	18.54	16.42	17.645
^{215}Pa	^{211}Ac	8.235	− 3.15	− 2.63	− 2.34	− 2.85	− 1.854
^{217}Pa	^{213}Ac	8.488	− 3.90	− 3.44	− 3.15	− 3.56	− 2.444
^{218}Pa	^{214}Ac	9.815	− 7.13	− 7.00	− 6.71	− 6.58	− 3.947
^{222}Pa	^{218}Ac	8.895	− 5.07	− 4.71	− 4.42	− 4.66	− 2.538
^{223}Pa	^{219}Ac	8.325	− 3.56	− 3.07	− 2.77	− 3.25	− 2.292
^{224}Pa	^{220}Ac	7.693	− 1.68	− 1.03	− 0.73	− 1.46	− 0.073
^{225}Pa	^{221}Ac	7.395	− 0.71	0.02	0.31	− 0.54	0.230
^{226}Pa	^{222}Ac	6.987	0.74	1.57	1.86	0.85	2.033
^{227}Pa	^{223}Ac	6.580	2.33	3.26	3.56	2.37	3.361
^{231}Pa	^{227}Ac	5.150	9.49	10.78	11.07	9.30	12.015
^{226}U	^{222}Th	7.701	− 1.33	− 0.67	− 0.35	− 1.16	− 0.572
^{228}U	^{224}Th	6.803	1.87	2.74	3.07	1.89	2.737
^{230}U	^{226}Th	5.992	5.78	6.86	7.18	5.67	6.255
^{232}U	^{228}Th	5.414	8.44	9.66	9.99	8.24	9.337
^{233}U	^{229}Th	4.909	11.56	12.91	13.24	11.28	12.701
^{234}U	^{230}Th	4.857	11.90	13.26	13.58	11.61	12.889
^{235}U	^{231}Th	4.678	13.14	14.55	14.87	12.82	16.346
^{236}U	^{232}Th	4.573	13.90	15.33	15.66	13.56	14.868
^{236}Pu	^{232}U	5.867	6.93	8.04	8.43	6.69	7.955
^{238}Pu	^{234}U	5.593	8.37	9.55	9.93	8.08	9.442
^{239}Pu	^{235}U	5.245	10.40	11.67	12.05	10.06	11.881
^{240}Pu	^{236}U	5.256	10.38	11.64	12.03	10.04	11.316
^{238}Am	^{234}Np	6.040	6.52	7.58	8.00	6.24	3.769
^{239}Am	^{235}Np	5.922	7.10	8.19	8.61	6.81	4.632
^{241}Am	^{237}Np	5.638	8.59	9.75	10.17	8.25	10.135
^{243}Am	^{239}Np	5.439	9.69	10.91	11.33	9.32	11.366
^{240}Cm	^{236}Pu	6.398	5.25	6.23	6.67	4.98	6.368
^{242}Cm	^{238}Pu	6.216	6.07	7.09	7.54	5.77	7.148
^{243}Cm	^{239}Pu	6.169	6.28	7.31	7.76	5.97	8.963
^{244}Cm	^{240}Pu	5.902	7.62	8.72	9.16	7.26	8.756
^{247}Bk	^{243}Am	5.890	8.13	9.23	9.71	7.72	10.639
^{242}Cf	^{238}Cm	7.517	1.55	2.25	2.76	1.34	2.321
^{244}Cf	^{240}Cm	7.329	2.21	2.95	3.46	1.97	3.066
^{250}Cf	^{246}Cm	6.128	7.34	8.39	8.90	6.91	8.615
^{251}Cf	^{247}Cm	6.177	7.08	8.11	8.62	6.65	10.452
^{252}Cf	^{248}Cm	6.217	7.07	8.09	8.60	6.65	7.921
^{253}Es	^{249}Bk	6.739	4.89	5.78	6.33	4.50	6.248
^{252}Fm	^{248}Cf	7.153	3.63	4.41	4.99	3.24	4.961
^{254}Fm	^{250}Cf	7.307	2.98	3.73	4.31	2.62	4.067
^{255}Fm	^{251}Cf	7.240	3.23	3.99	4.57	2.86	4.859
^{257}Fm	^{253}Cf	6.863	4.74	5.60	6.18	4.31	6.939
^{254}No	^{250}Fm	8.226	0.55	1.08	1.71	0.22	1.708
^{256}No	^{252}Fm	8.581	− 0.60	− 0.16	0.47	− 0.87	0.464

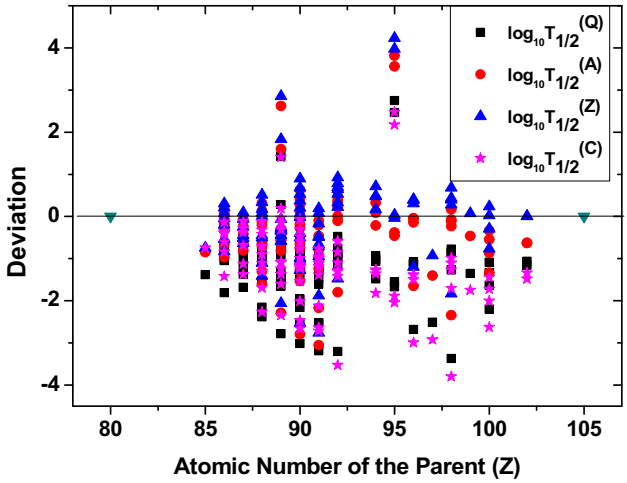

Figure 6. Deviation between logarithm of the predicted values and experimental values for alpha decay from different parent nuclei.

Standard deviations of logarithm of half-lives in seconds, $T_{1/2}^{(Q)}$, $T_{1/2}^{(A)}$, $T_{1/2}^{(Z)}$, $T_{1/2}^{(C)}$, are found to be 1.08, 0.995, 1.07 and 0.885 respectively. Thus, it is evident that our model provides reasonable results that can explain cluster emission.

In table 7, we extend our work, by applying the same pre-formation probabilities in the case of alpha particle considering it as the lightest cluster. Half-lives of alpha particles emitted from parent nuclei with atomic number 85–102 are calculated and compared with experimental values. To understand the exact matching between experimental and theoretical results, a graph is plotted with atomic number of the parent nuclei along the X-axis and difference of logarithm of the theoretical and experimental half-lives on the Y-axis as shown in figure 6. Black rectangle, red circle, blue triangle and pink star in the figure show the half-lives corresponding to Q value-dependent, cluster size-dependent, product of atomic number of the cluster and the daughter-dependent pre-formation factor and with combined pre-formation factor respectively. Majority of difference of logarithmic half-lives lies within the range of -2 to 1, showing less deviation of the predicted half-life from the experimental values. These results with better accuracy in the case of alpha decay again prove the validity of our model.

In the present paper, we have deduced three expressions for pre-formation factor after verifying the dependence of pre-formation factor on Q value, mass cluster size and product of the atomic numbers of the cluster and the daughter nuclei and is shown in figure 1. Since the dependence is evident from the graph, we have deduced three separate formulae to check the predictive power in each case. Predictive power will be more when the standard deviation by the formulae is the least. In the present study, predictive power is more for cluster size-dependent pre-formation factor with a standard deviation of 0.995 than with the other two formulae.

In our earlier work [45], we checked the dependence of pre-formation factor on Q value. But in the present paper which is an extension of [45], not only Q value dependence of the pre-formation factor, but also all the other dependences like cluster size, product of the atomic numbers of the cluster and the daughter nuclei are also checked. As a final interesting factor, new formulae for the pre-formation factor, combining all the three dependence terms, is deduced in this paper which could reproduce experimental values well with high predictive power.

4. Conclusions

Cluster decay half-lives of trans-lead nuclei using MGLDM with four types of pre-formation factors which depend on Q value, size of the cluster, product of proton number of the cluster and the daughter and also with a pre-formation factor containing all three factors together in an expression are studied. Theoretically predicted results are made to compare with experimental values and a better matching was obtained. Standard deviations for logarithmic half-lives (about 1.08, 0.995, 1.07 and 0.885) were obtained with the above stated pre-formation factor. The predictive power with the formulae containing combined pre-formation factor is the highest. And the same four formulae are applied in the case of alpha decay which could replicate the observed values. Thus, one could clearly suggest that the present

model is applicable to both cluster and alpha decay processes.

Acknowledgements

One of the authors (KPS) would like to thank the Government of Kerala, India for the financial support in the form of Research Project under Innovative Research Programme.

References

[1] A Sandulescu, D N Poenaru and W Greiner, *Sov. J. Part. Nucl.* **11**, 528 (1980)
[2] H J Rose and G A Jones, *Nature* **307**, 245 (1984)
[3] D V Aleksandrov, A F Belyatskii, Y A Glukhov, E Y Nikolskii, B G Novatskii, A A Ogloblin and D N Stepnov, *JETP Lett.* **40**, 909 (1984)
[4] R K Gupta and W Greiner, *Int. J. Mod. Phys. E* **3**, 335 (1994)
[5] Y S Zamyatnin, V L Mikheev, S P Tret'yakova, V I Furman, S G Kadmenskii and Y M Chuvil'skii, *Sov. J. Part. Nucl.* **21**, 231 (1990)
[6] P B Price, *Annu. Rev. Nucl. Part. Sci.* **39**, 19 (1989)
[7] E Hourani, M Hussonnois and D N Poenaru, *Ann. Phys. (Paris)* **14**, 311 (1989)
[8] S S Malik, S Singh, R K Puri, S Kumar and R K Gupta, *Pramana – J. Phys.* **32**, 419 (1989)
[9] D N Poenaru, W Greiner, M Ivascu and A Sandulescu, *Phys. Rev. C* **32**, 2198 (1985)
[10] S W Barwick, P B Price and J D Stevenson, *Phys. Rev. C* **31**, 1984 (1985)
[11] P B Price and K J Moody, *Phys. Rev. C* **46**, 1939 (1992)
[12] R Bonetti, C Carbonini, A Guglielmetti, M Hussonnois, D Trubert and C Le Naour, *Nucl. Phys. A* **686**, 64 (2001)
[13] S Kumar, M Balasubramaniam, R K Gupta, G Münzenberg and W Scheid, *J. Phys. G: Nucl. Part. Phys.* **29**, 625 (2003)
[14] S Kumar, R Rani and R J Kumar, *J. Phys. G: Nucl. Part. Phys.* **36**, 015110 (2009)
[15] M Balasubramaniam and R K Gupta, *Phys. Rev. C* **60**, 064316 (1999)
[16] D N Poenaru, M Ivascu, A Sandulescu and W Greiner, *J. Phys. G: Nucl. Part. Phys.* **10**, L183 (1984)
[17] W Greiner, M Ivascu, D N Poenaru and A Sandulescu, *Z. Phys. A* **320**, 347 (1985)
[18] G Royer, R K Gupta and V Y Denisov, *Nucl. Phys. A* **632**, 275 (1988)
[19] G Royer and R Moustabchir, *Nucl. Phys. A* **683**, 182 (2001)
[20] G Royer and B J Remaud, *J. Phys. G: Nucl. Part. Phys.* **10**, 1057 (1984)
[21] G Royer and B Remaud, *Nucl. Phys. A* **444**, 477 (1985)
[22] G Royer, *J. Phys. G: Nucl. Part. Phys.* **26**, 1149 (2000)
[23] G Royer and R A Gherghescu, *Nucl. Phys. A* **699**, 479 (2002)
[24] G Royer, K Zbiri and C Bonilla, *Nucl. Phys. A* **730**, 355 (2004)
[25] H Zhang, W Zuo, J Li and G Royer, *Phys. Rev. C* **74**, 017304 (2006)
[26] G Royer and H F Zhang, *Phys. Rev. C* **77**, 037602 (2008)
[27] X J Bao, H F Zhang, B S Hu, G Royer and J Q Li, *J. Phys. G: Nucl. Part. Phys.* **39**, 095103 (2012)
[28] J Blocki, J Randrup, W J Swiatecki and C F Tsang, *Ann. Phys. (NY)* **105**, 427 (1977)
[29] K P Santhosh, S Krishnan and J G Joseph, *Pramana –J. Phys*. **91**: 5 (2018)
[30] K P Santhosh, C Nithya, H Hassanabadi and D T Akrawy, *Phys. Rev. C* **98**, 024625 (2018)
[31] R Blendowske, T Fliessbach and H Walliser, *Nucl. Phys. A* **464**, 75 (1987)
[32] S S Malik and R K Gupta, *Phys. Rev. C* **39**, 1992(1989)
[33] S Kumar, R K Gupta and W Scheid, *Int. J. Mod. Phys. E* **3**, 195 (1994)
[34] K Wei and H F Zhang, *Phys. Rev. C* **96**, 021601 (2017)
[35] D N Poenaru, M Ivascu, A Sandulescu and W Greiner, *Phys. Rev. C* **32**, 572 (1985)
[36] Y J Shi and W J Swiatecki, *Nucl. Phys. A* **464**, 205 (1987)
[37] F Barranco, G F Bertsch, R A Broglia and E Vigezzi, *Nucl. Phys. A* **512** 253 (1990)
[38] H F Zhang, J M Dong, G Royer, W Zuo and J Q Li, *Phys. Rev. C* **80**, 037307 (2009)
[39] R Blendowske and H Walliser, *Phys. Rev. Lett.* **61**, 1930 (1988)
[40] D Ni, Z Ren, T Dong and C Xu, *Phys. Rev. C* **78**, 044310 (2008)
[41] M Balasubramaniam and N S Rajeswari, *Int. J. Mod. Phys. E* **23**, 1450018 (2014)
[42] Z Ren, C Xu and Z Wang, *Phys. Rev. C* **70**, 034304 (2004)
[43] Y Qian and Z Ren, *J. Phys. G: Nucl. Part. Phys*. **39**, 015103 (2012)
[44] K P Santhosh and T A Jose, *Nucl. Phys. A* **992**, 121626 (2019)
[45] K P Santhosh and T A Jose, *Phys. Rev. C* **99**, 064604 (2019)
[46] K P Santhosh and C Nithya, *Phys. Rev. C* **97**, 064616 (2018)
[47] J Blocki and W J Swiatecki, *Ann. Phys. (NY)* **132**, 53 (1981)
[48] C Nithya, *Studies on modes of decay of normal and hypernuclei,* Ph.D. Thesis (Kannur University, 2019)
[49] G Audi, F G Kondev, M Wang, W J Huang and S Naimi, *Chin. Phys. C* **41**, 030001 (2017)